

archives
of thermodynamics

Vol. 44(2023), No. 1, 23–36

DOI: 10.24425/ather.2023.145875

Thermodynamics-based measurement of the velocity of high-temperature smoke

HAOYU WANG*

Department of Fire Engineering, China Fire and Rescue Institute,
Nanyan 4, Changping District, 102202, Beijing; China

Abstract In view of the high cost and difficulty of ensuring the accuracy in the measurement of fire smoke velocity, the measurement system developed using platinum resistance temperature detectors and an 8-bit microcontroller, is used to realize the fast measurement of high-temperature fire smoke velocity. The system is based on the thermodynamic method and adopts the Kalman filter algorithm to process the measurement data, so as to eliminate noise and interference, and reduce measurement error. The experimental results show that the Kalman filter algorithm can effectively improve the measurement accuracy of fire smoke velocity. It is also shown that the system has high measurement accuracy, short reaction time, low cost, and is characterized by high performance in the measurement of high-temperature smoke velocity in experiments and practice.

Keywords: Thermodynamics; Smoke; Flow velocity; Measurement; Kalman filter algorithm

Nomenclature

- η – Einstein coefficient
- C_p – specific heat capacity, J/kgK
- l – distance between two temperature detectors, m
- q – heat flux density, J/m²

*Corresponding Author. Email: taofuyanuk119@163.com

- r – radius of the tube, m
- x – state variable
- v – flow rate of the measured gas, m/s
- ρ – density, kg/m³

Greek symbols

- η – Einstein coefficient

1 Introduction

The smoke spreading in fire buildings poses a fatal threat to indoor personnel. The research on smoke flow and control in buildings has attracted extensive attention [1]. The smoke velocity as an important parameter of smoke movement is commonly referred to in related studies and is worth measuring. However, it is difficult to obtain the velocity of high-temperature smoke due to the smoke heat and the blockage and erosion caused by numerous carbon black particles and droplets [2]. Two types of smoke velocity measurement are mainly adopted, one is based on the pressure difference with a pitot tube, and the other is based on a leveraged hot-wire device [3]. The Pitot tube, is conducive to measuring high flow rates, and the error will be greater at low flow rates [4]; the accuracy of the hot-wire device is high, but the probe is prone to be blocked and damaged by the carbon black particles in the smoke. The probe price is high, and the damage of the probe will greatly increase the experimental cost. Hence, finding a low-cost, applicable and reliable measurement method is necessary. Zhou *et al.* [5] proposed an approach to measure the smoke velocity by using the temperature pulse information of smoke. This method used the polarity correlation technology to process temperature data with a short response time and high accuracy, but the measurement was limited by the distance from the fire source and the severity of combustion. The error was even larger when the fire source was far away or the combustion remained relatively stable. Shen *et al.* [6] utilized thermodynamics to measure the coal flow rate in coal-fired boiler pneumatic conveying. However, the measurement of smoke velocity by the thermodynamic method has a large error. To improve the accuracy, the data filtering technology can be used to eliminate the noise and interference in measurement, so as to restore the real data and improve the measurement accuracy.

The principles of the thermodynamic method and Kalman filter algorithm are introduced first; then the structure of the thermodynamics-based velocity measurement system is presented, and the measurement results with the hot wire equipment are compared. Finally, the conclusions are given.

2 The measurement principle of thermodynamics

The measurement principle is demonstrated in Fig. 1. The smoke flows from the combustion chamber into the velocity measuring tube, the middle of which is heated by a fixed heat source. The measurement system is composed of two probes, a signal converter and a microcontroller. The velocity probes are made of platinum resistance temperature detectors, one of which measures the smoke temperature as T_1 , the other is heated to a temperature higher than the smoke as T_2 .

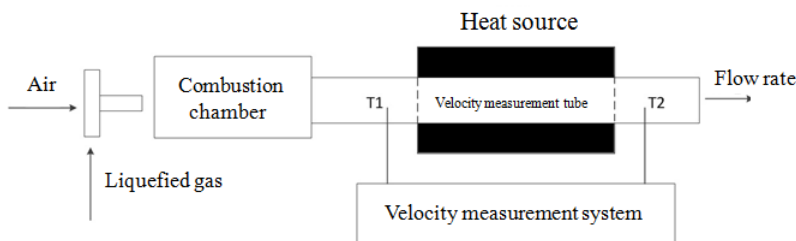


Figure 1: Measuring principle of smoke velocity based on thermodynamics.

According to the principle of heat transfer and energy conservation

$$C_p \rho v \pi r^2 (T_2 - T_1) = q 2\pi r l, \quad (1)$$

where C_p is the specific heat capacity of the smoke, ρ is the smoke density, v is the flow rate of the measured gas, r is the radius of the tube, q is the heat flux density of the heat source, and l is the distance between two platinum resistances temperature detectors.

From Eq. (1), we have

$$\Delta T = T_2 - T_1 = \frac{2ql}{C_p r} \frac{1}{\rho v}. \quad (2)$$

Since the smoke density varies little in the actual measurement environment, the flow rate of the measured smoke can be calculated through the measurement of the temperature difference (ΔT) from above relationship [7].

3 The mechanism of the Kalman filter

The Kalman filter is an algorithm that uses the state equation of a linear system to optimally estimate the system through the input and output observation data [8]. To make the measurement result closer to the real data, the Kalman filter algorithm introduces the state variable formula and adds the changing noise to the formula to compensate for the unpredictable error. The state variable in the Kalman filter algorithm can be expressed as follows:

$$x_k = \mathbf{A}x_{k-1} + \mathbf{B}u_{k-1} + w_{k-1}, \quad (3)$$

where x is the filtered state variable; \mathbf{A} is the state matrix; u is the control variable; \mathbf{B} is the control matrix; w is the process noise, and k represents the k th process.

The measurement results calculated by the thermodynamic method can be expressed as follows:

$$z_k = \mathbf{H}x_k + y_k, \quad (4)$$

where z is the result of thermodynamic measurement; \mathbf{H} is the gain matrix, x is the variable of state, and y is the measurement noise. Due to the error of z , it cannot be directly used as a measurement result, and it needs to be converted into a state variable through the gain matrix \mathbf{H} .

The distribution of the process noise w and the measurement noise v in the algorithm can be expressed by relations:

$$p(w) \sim N(0, Q), \quad (5)$$

$$p(v) \sim N(0, R), \quad (6)$$

where p and N , representing the process noise and observation noise, are independent, and follow normal distribution from 0 to Q and 0 to R , respectively. In a real system, the process noise covariance matrix \mathbf{Q} and the observation noise covariance matrix \mathbf{R} change with each iteration [9].

The filtering process of the Kalman filter algorithm is shown in Fig. 2 [10].

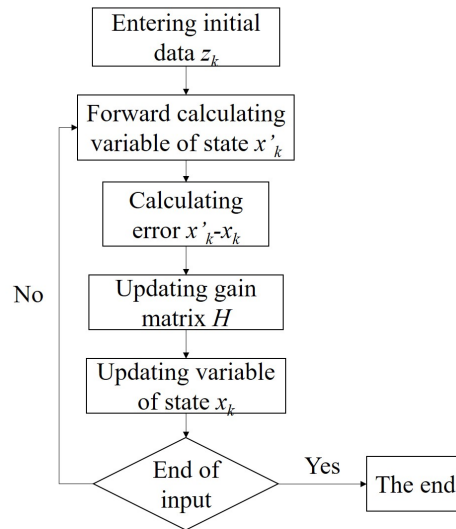


Figure 2: Flow chart of the Kalman filter algorithm.

4 The velocity component measurement system

The hardware of the velocity measurement system mainly includes two platinum resistance temperature detectors Pt100, a data acquisition module, a velocity display screen and an 8-bit microcontroller (MCU) 8051, as shown in Fig. 3. The temperature measurement range of the Pt100 resistance tem-

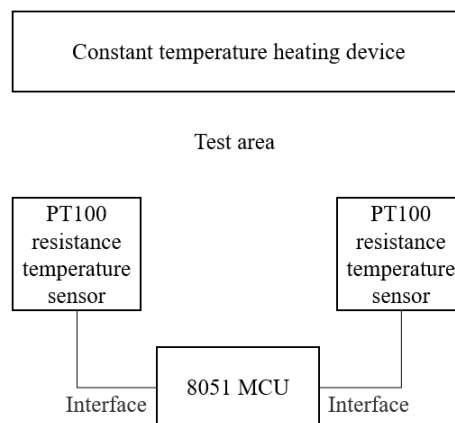


Figure 3: Structure of the velocity measurement system.

perature sensor is $0\text{--}550^\circ$, which meets the experimental requirements. The sensor also has the advantages of anti-vibration, corrosion resistance, optimal stability and high accuracy. In addition, compared with the probe of the hot wire device, the probe of the sensor is a closed structure, which will not be blocked by smoke particles and is easy to clean. 8051 MCU is widely used in data acquisition and processing.

The system software is written in 8051 MCU C language and consists of two modules: real-time data acquisition and velocity calculation display. The Kalman filter algorithm is adopted for data processing. The data acquisition frequency is 1000 Hz; the measurement range is $0\text{--}20$ m/s; the accuracy is 0.1 m/s, and the error is $\pm 10\%$. The data acquisition time of the system is 2 s; the calculation time is 3 s, and the total response time is less than 5 s, which is in accordance with the response time required in experiments and actual measurements.

5 Experimental results and analysis

The smoke velocity measurement experiments were carried out in a $1/3$ scale simulated high-rise building, as shown in Figs. 4–6. The experimental house has 10 storeys, each with a storey height of 1 m. The mixture of liquefied petroleum gas (LPG) and the air was burned in the experimental room, producing high-temperature smoke. Then the smoke entered the corridor through the open door. The flow rate and temperature of the smoke were adjusted by changing the flow rate of liquefied gas and air. Considering the size of the fire source and the smoke velocity, the horizontal corridor directly

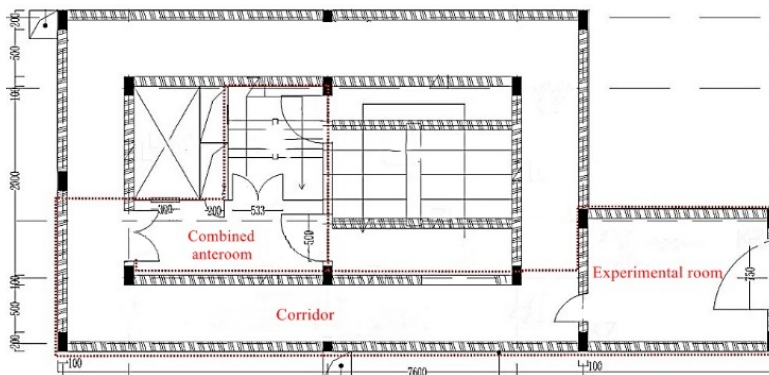


Figure 4: $1/3$ scale fire experiment house plan.

connected with the experimental room on the third floor was selected as the velocity measurement section of the experiment. The schematic diagram of the chosen ‘room-corridor’ section is illustrated in Fig. 7.



Figure 5: The northern side of the experimental house.



Figure 6: The southern side of the experimental house.

To verify the accuracy of the measurement results, a handheld high-temperature anemometer (model 6162) manufactured by Kanomax, was selected for simultaneous measurement at the same measuring point. Then the results of the measurement system and the anemometer are compared. The anemometer includes a host and a probe, which is suitable for two types of probes, the medium-temperature model 0203 and the high-temperature

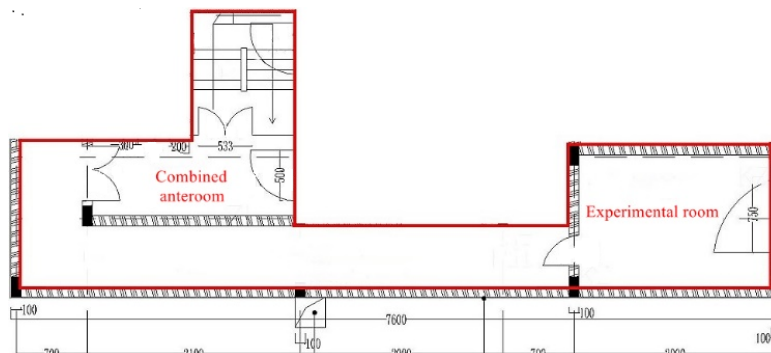


Figure 7: The 'room-corridor' plan of the experiment.

model 0204. The experiment used the high-temperature model 0204 probe, and the host response time was less than 4 s.

Before the experiment, the equipment was calibrated under normal temperature and 0.5 m/s wind speed, and the results are shown in Fig. 8. It shows that the measurement results are basically consistent at room temperature and constant wind speed.

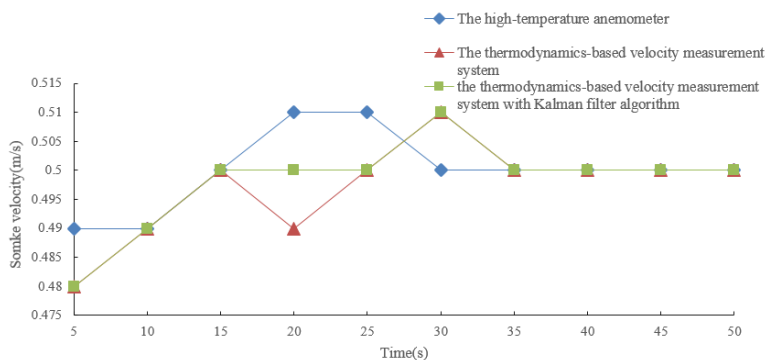


Figure 8: Results of the calibration test.

Two comparative experiments were conducted in total. The measuring point of the first experiment was located at a horizontal distance of 3.2 m from the corridor to the experimental room (the room of fire origin), and a vertical distance from the corridor floor of 0.85 m. The measuring point of the second experiment was located at a horizontal distance of 4.2 m from the corridor to the experimental room, and a vertical distance from the corridor floor of 0.85 m. According to the similarity criterion of the physical

model, the scale of the distance and height of the 1/3 scale simulated high-rise building experiment house to the actual size is 1 to 3. To this end, the actual location of the measuring points is 9.6 m and 12.6 m of horizontal distance from the room, and the vertical height is 0.45 m under the ceiling. The smoke velocity is relatively stable and is convenient for measurement. The data collection cycle is 5 s. The results of the first experiment are shown in Figs. 9 and 10.

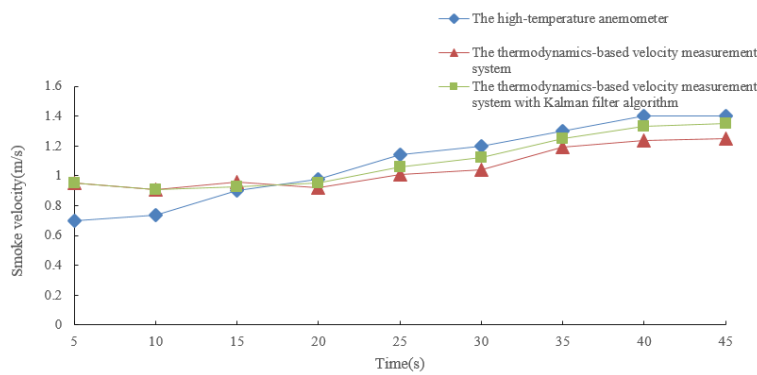


Figure 9: Results of the first experiment.

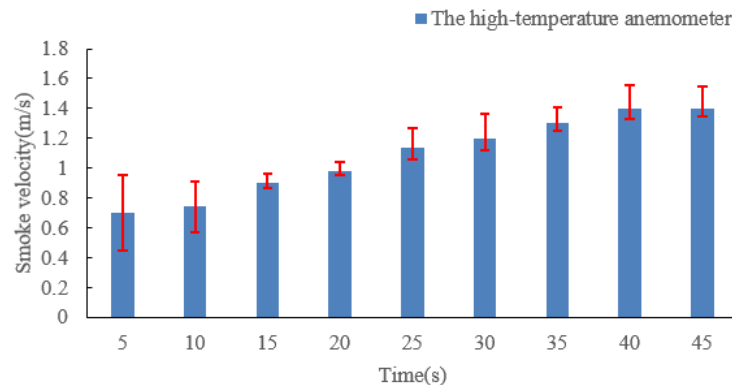


Figure 10: Error analysis of the first experiment.

Figure 9 illustrates the comparison of the measurement results from the two methods, and Fig. 10 displays the error diagram of the thermodynamics-based velocity measurement system with the Kanomax model 6162 hand-held anemometer as the standard. The upper end of the error line is the

direct measurement result based on the thermodynamic method, and the lower end is the measurement result of the software system obtained with the Kalman filter algorithm. It can be seen that the measurement results of the smoke velocity of the Kalman filter algorithm at the same location are closer to those of the handheld high-temperature anemometer. At the beginning of the experiment, the deviation between the two measurement systems is relatively large, but the results tend to be consistent after 15 s. This is because the Kalman filter algorithm needs to receive initial data for iterative calculations to eliminate noise and interference at the beginning of the measurement. After that, the change of the gain matrix tends to be stable, and the measurement accuracy is significantly improved. Compared with the handheld anemometer, the average deviation of the measurement results of the thermodynamic method is 9.9%, and that processed by the Kalman filter algorithm is 6.6%, improved by 33.3%.

The measurement results of the second experiment are shown in Figs. 11 and 12. Figure 11 shows the comparison of the measurement results of the two methods. Figure 12 shows the error diagram of the thermodynamics-based velocity measurement system based on the Kanomax model 6162 handheld anemometer. The upper end of the error line is the direct measurement results based on the thermodynamic method, and the lower end is the measurement results of the software system with the Kalman filter algorithm. As shown in Figs. 11 and 12, the measurement results of smoke velocity with the Kalmanfilter algorithm at the same location are closer to those of the handheld high-temperature anemometer. At the beginning of the experiment, the deviation between the two measurement systems is

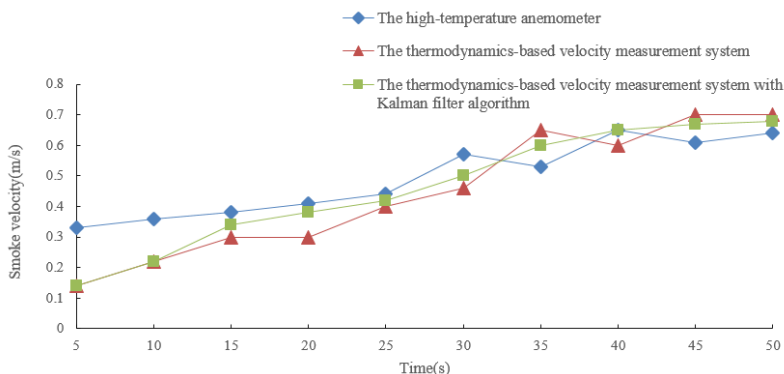


Figure 11: Results of the second experiment.

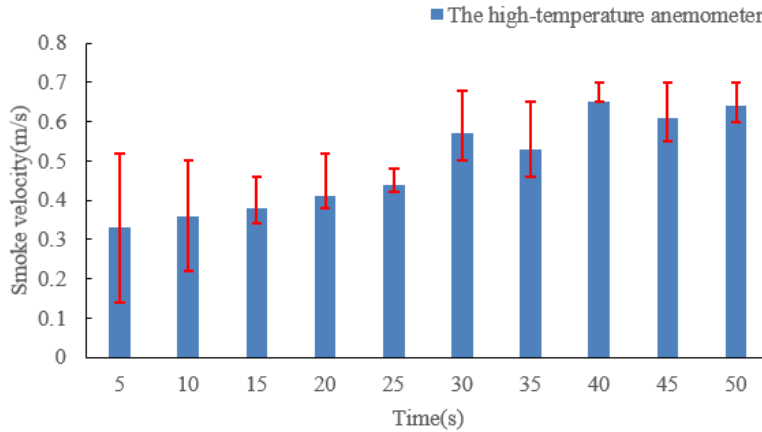


Figure 12: Error analysis of the second experiment.

relatively large, and the results tend to be consistent after 15 s. Compared with the handheld anemometer, the average deviation of the measurement results based on the thermodynamic method is 13.89%, and that based on the Kalman filter algorithm is 9%, improved by 35.2%.

In the initial stage of the experiment, the temperature in the corridor was low; the Pt100 resistance value was large, and the signal value generated in the circuit was too small, resulting in large errors [11, 12]. As the experiments progressed, the temperature in the corridor gradually increased; the platinum resistance value decreased, and the signal value in the circuit increased. The accuracy of the system was improved. Since the Kalman filter algorithm needs initial data for iterative calculation in the initial stage, it cannot effectively eliminate the error in this stage.

Due to the differentials in the algorithms and types of probes in the two experiments, as well as the diversity of smoke particles and the complexity of motions, the deviation between the thermodynamics-based measurement results and the high-temperature anemometer measurement results is still within the acceptable range in the actual gauge. Although the measurement accuracy in the low temperature area is not satisfying, the thermodynamics-based smoke velocity measurement system has relatively high accuracy from the overall perspective.

In addition, the experiments show that the data sampling frequency will affect the measurement accuracy [13]. The measurement accuracy can be optimized by increasing the sampling frequency, and the sampling fre-

quency cannot be increased indefinitely due to the limitation of hardware conditions [14]. When the sampling frequency is 1000 Hz, the measurement accuracy can meet the measurement requirements under general experimental conditions. The experiments show that the data acquisition time will also affect the measurement accuracy. The longer is the data acquisition time, the higher is the measurement accuracy. Due to the limitations of hardware conditions and response time requirements, the data acquisition time cannot be too long [15]. When the data acquisition time is 2 s, higher measurement accuracy can be available, and the response time of the system is also within an acceptable range.

6 Conclusions

The velocity of high-temperature smoke was measured by the thermodynamic method, and the results demonstrate that the system has high accuracy and measurement precision. The results show that:

1. The Kalman filtering algorithm effectively improves the accuracy of measuring smoke velocity by the thermodynamic method.
2. Compared with the handheld high-temperature anemometer, the accuracy of the thermodynamic smoke velocity measurement system based on the Kalman filter algorithm can meet the requirements of experimental measurement, and the system has lower cost and higher equipment reliability.
3. At the beginning of the experiment, the results of the measurement system based on the thermodynamic method have a larger deviation than that of the handheld high-temperature anemometer. Due to the characteristics of the algorithm, the Kalman filter algorithm has no obvious effect at this stage. This error needs to be further corrected by a neural network model with more test data.
4. When the data sampling frequency is 1000 Hz and the acquisition time is 2 s, the accuracy of the smoke velocity measurement system reaches 0.1 m/s.

It is worth noting that the error of the system at low temperatures is larger than that at high temperatures. Although the response time can

meet most experimental requirements, there is still room for further improvement. These problems need to be further solved in the follow-up study.

Received 18 November 2022

References

- [1] Trawiński P.: *Development of real gas model operating in gas turbine system in Python programming environment*. Arch. Thermodyn. **41**(2020), 4, 23–61. doi: [10.24425/ather.2020.135853](https://doi.org/10.24425/ather.2020.135853)
- [2] Shibata K., Shimizu M., Inaba S.I., Takahashi R., Yagi J.I.: *One-dimensional flow characteristics of gas-powder two phase flow in packed beds*. Tetsu-to-Hagane **77**(1991), 2, 236–243 (in Japanese). doi: [10.2355/tetsutohagane.1955.77.2_236](https://doi.org/10.2355/tetsutohagane.1955.77.2_236)
- [3] Pan L.W.: *On the characteristics of smoke stratified transportation with smoke control in tunnel*. Univ. Sci. Technol. China, Hefei 2011 (in Chinese).
- [4] Nguyen D.T., Choi Y.M., Lee S.H., Kang W.: *Experimental investigation on the optimum geometry of an s-type pitot tube for GHG emission monitoring*. J. Phys. Conf. Ser. **1065**(2018), 9, 092009. doi: [10.1088/1742-6596/1065/9/092009](https://doi.org/10.1088/1742-6596/1065/9/092009)
- [5] Zhou J., Yuan Z.F., Pu X.G., Wang K., Lu Y.G., Cen K.F.: *Study of zero-crossing polarity correlation for velocity measurement of high temperature flue gas*. Proc. CSEE **19**(1999), 3, 12–14. doi: [10.3321/j.issn:0258-8013.1999.03.003](https://doi.org/10.3321/j.issn:0258-8013.1999.03.003)
- [6] Shen A., Sun Z.K., Zhou L., Hu B., Yuan Z.L., Yang L.J.: *Experimental study on coupling of turbulent and chemical agglomeration to promote coal particles removal by electrostatic precipitator*. Proc. CSEE **39**(2019), 10, 2954–2962. doi: [10.13334/j.0258-8013.pcsee.180842](https://doi.org/10.13334/j.0258-8013.pcsee.180842)
- [7] Joachimiak M., Joachimiak D., Krzyślak P.: *Analysis of heat flow in a tube bank of a condenser considering the influence of air*. Arch. Thermodyn. **38**(2017), 3, 119–134. doi: [10.1515/aoter-2017-0019](https://doi.org/10.1515/aoter-2017-0019)
- [8] Xue C., Huang Y., Zhu F., Zhang Y., Chambers J.A.: *An outlier-robust Kalman filter with adaptive selection of elliptically contoured distributions*. IEEE T. Signal Process. **70**(2022), 994–1009. doi: [10.1109/TSP.2022.3151199](https://doi.org/10.1109/TSP.2022.3151199)
- [9] Cai W., Nasser B.B., Djemai M., Laleg-Kirati T.M.: *Kalman filter design for intermittent optical wireless communication systems on time scales*. arXiv prep. arXiv:2203.16166[eess.SY], (2022). doi: [10.48550/arXiv.2203.16166](https://doi.org/10.48550/arXiv.2203.16166)
- [10] Gonzalez-Cagigal M.A., Rosendo-Macias J.A., Gomez-Exposito A.: *Parameter estimation of fully regulated synchronous generators using unscented Kalman filters*. Electr. Pow. Syst. Res. **168**(2019), 210–217. doi: [10.1016/j.epsr.2018.11.018](https://doi.org/10.1016/j.epsr.2018.11.018)
- [11] Treichel Z., Dabrowski D., Peryt M., Roslon K.: *Verification of operation Pt100 platinum resistance thermometer to measure the electronic elements inside time-of-flight (TOF) detector*. Acta Phys. Pol. B Proc. Suppl. **11**(2018), 4, 759–764. doi: [10.5506/APHYSPOLBSUPP.11.759](https://doi.org/10.5506/APHYSPOLBSUPP.11.759)

-
- [12] Ruan C.Z.: *A design of temperature measurement system based on Pt100 resistance*. J. Wuyi Univ. **33**(2014), 2, 62–65. doi: [10.14155/j.cnki.35-1293/g4.2014.02.013](https://doi.org/10.14155/j.cnki.35-1293/g4.2014.02.013)
- [13] Zhang H., Guo C.S., Chen Y.: *Inverse material characterization through finite element simulation of material tests and numerical optimization*. Procedia Manuf. **34**(2019), 455–462. doi: [10.1016/j.promfg.2019.06.198](https://doi.org/10.1016/j.promfg.2019.06.198)
- [14] Wang H.Q., Wang Y.H., Ren S.T., Meng Q.T., Wang Y.L.: *Research on frequency response characteristics of ring type electrostatic sensor for gas-solid two-phase flow detection*. Laser Optoelectron. Prog. **57**(2020), 17, 149–154. doi: [10.3788/LOP57.171202](https://doi.org/10.3788/LOP57.171202)
- [15] Hu H.L., Tang K.H., Tang C.H., Wang X.X.: *Fundamentals of electrical capacitance sensing and its applications for two-phase flow parameter detection*. J. Northwest Univ. (Nat. Sci. Edn.) **49**(2019), 681–690. doi: [10.16152/j.cnki.xdxbzr.2019-05-002](https://doi.org/10.16152/j.cnki.xdxbzr.2019-05-002)